Noname manuscript No.
(will be inserted by the editor)

Excitation-power independent Photoluminescence of Inverted-Quantum-Hut Structures embedded in SiGe superlattice

Manjula Sharma, Milan K. Sanyal, Ajit Katiyar and Samit K. Ray

Received: date / Accepted: date

Abstract Optical properties of semiconductor nanostructures can be quite different from the bulk semiconductors. We present here results of a photoluminescence study of MBE grown SiGe superlattice structures having inverted quantum huts of Ge formed below Ge-on-Si interfaces. As these structures form by continuous alloying with the lower Si layers, the interfacial strain is greatly reduced, leading to a band-alignment which is different from that obtained for conventional quantum dots formed above Ge-on-Si interfaces. Thus, unlike conventional Ge quantum dots, the presented quantum structures exhibit excitation-power independent photoluminescence emission. Temperature dependence of photoluminescence energy follow typical relation expected in a semiconductor but at higher temperature when dominating contribution comes from the tip of the quantum hut, change in the photoluminescence energy becomes weakly dependent on temperature. These results may be influential in the development of silicon based optical materials.

Keywords Silicon-photonics · Silicon-Germanium superlattice · Quantum structure · Photoluminescence

M. Sharma and M. K. Sanyal
Surface Physics and Materials Science Division, Saha Institute of Nuclear Physics, 1/AF Bidhannagar, Kolkata, 700064, India.
Tel.: +91-033-23214763
Fax: +91-033-23374637
E-mail: milank.sanyal@saha.ac.in

A. Katiyar and S. K. Ray
Department of Physics and Meteorology, Indian Institute of Technology Kharagpur, Kharagpur, 721302, India.

1 Introduction

Indirect-gap semiconductor materials like silicon or germanium show poor light emission properties as the momentum wave-vectors of the conduction band minima and valence band maxima are at different positions in k-space requiring inefficient phonon-assisted radiative recombination processes. However, excitons in nanostructures can be quite different and enormous amount of research is being done to embed suitable nanostructures (particularly germanium quantum dots) in silicon, to develop Si-based light emitting material for semiconductor industry [1–3]. But pseudomorphic growth of Ge (having 4% bigger lattice parameter than Si) quantum dots on Si (001) surface and subsequent capping with Si generate inherent interfacial strain in these materials [4, 5]. The presence of strain at the interface of Ge quantum dot and Si (001) lattice leads to complicated energy-band alignment hindering development of efficient silicon based optical materials as transition remains Type-II, showing strong dependence of photoluminescence (PL) on excitation power [6–10]. Here we show that Ge inverted quantum hut structures grown within Si (001) crystals reduce importance of the interfacial strain and exhibit strong PL whose energy remains almost independent of the excitation power.

In conventional growth of Ge over Si (001) by molecular beam epitaxy (MBE) technique, first few monolayers form a wet layer followed by the formation of 3-D nanostructures i.e. quantum dots (QD) of Ge to relax the accumulated strain due to the lattice mismatch [4, 5]. These quantum dots with tip pointing up are then overgrown by Si capping in order to avoid oxidation and surface recombination of exciton for the development of a Si based optical material. Recent experiments have shown that at low temperature growth of Si/Ge multi-

layers, inverted quantum hut (IQH) structures form below the Ge wet-layer with their apex pointing towards Si substrate [11–13]. X-ray diffraction results [13] have shown that at low growth temperature ($< 500°$C), Ge atoms have lower in-plane diffusivity and hence strain relaxation occurs by interdiffusion with the lower Si layers. During this interdiffusion, atom replacement occurs leading to SiGe alloy formation which lowers the interfacial strain considerably. Unlike conventional Ge QD structures, here we show that these IQH structures exhibit very small (around 2meV) shift in emitted PL at 0.81eV as a function of excitation power.

2 Experiment

The 10 bilayer Si/Ge superlattice structure was deposited in a solid-source molecular beam epitaxy (MBE) system at a growth temperature of 400°C at a base pressure of 10^{-11} Torr. Si and Ge were grown in same UHV chamber with identical growth condition. A Si buffer layer of 100nm thickness was first deposited on Si (001) substrate, then the 10 bilayer Si/Ge superlattice structure with nominal layer thicknesses of 70/20Å respectively, was grown followed by a Si cap layer of 300Å. Figure 1(a) is a cross-sectional high angle annular dark field (HAADF) image showing the Si/Ge superlattice consisting of IQH structures. The dark region in the HAADF image signifies the presence of Si while the lighter ones represent the presence of Ge. As can be seen in Figure 1(a), the dark lines have higher thickness and the lighter ones have lower thickness hence, Si/Ge layer thicknesses are consistent with what has been provided. Figure 1(b) shows the high resolution cross-sectional transmission electron microscope (XTEM) image of *Ge*-IQH structures present in the Si/Ge superlattice. The dark region here represents the presence of Ge and lighter region shows Si. The triangular regions having high contrast are the Ge-IQH structures having their apex towards the Si buffer layer. These Ge-IQH are observed to be self-organized one over the other in various Ge layers in the superlattice. The superlattice period of 90 Å can easily be estimated from the portion apart from the Ge-IQH.

The process of the formation of IQH structures has been studied in detail by anomalous x-ray scattering for a similar Si/Ge superlattice structure [13]. It was shown that the deposited Ge layer relaxes strain by diffusing into the previously deposited lower Si layer to form a $Si_{0.6}Ge_{0.4}$ wet layer and IQH structure form below it. The IQH structures are found to be completely epitaxial and do not consist of any misfit dislocations as can be confirmed from Figure 1(b). These IQH can be considered to be made up of circular disks with disk-diameter decreasing as one move from the base to the tip of the IQH. Each disk is assigned to a different in-plane lattice parameter ($a_{\|}$) depending upon the composition and strain relaxation at that position within the IQH. Since, the density of the IQHs present in the superlattice system is very low [refer Figure 1(a)] and we intend to find the lateral size of these IQH, grazing incidence diffraction technique was used to improve the surface sensitivity. The x-ray measurements were performed at P08 beamline of Petra III, Germany. The x-ray energy used was 11 043eV and the incident angle was fixed at 0.1°. Figure 1(c) shows typical angular scans in the vicinity of Si (400) diffraction peak. The z-axis is related to the measured intensity and the two in-plane axes (x and y) correspond to angular momentum transfer and the in-plane lattice parameter respectively. The scans are sensitive to different $a_{\|}$ and hence each scan corresponds to a particular disk in our model [refer Figure 1(c)]. The line profiles plotted with each angular scan data (represented by spheres) are the theoretical fits which provide the lateral extent (or diameter) of each disk. The measurements and data fitting have been carried out following a previous study [13]. The primary results obtained from x-ray analysis are shown schematically in Figure 1(d). As can be observed from the low magnification HAADF image [refer Figure 1(a)], there is a variation in the size of various IQHs and we have indicated this with two sizes of IQH in Figure 1(d). The wet layer thickness obtained from x-ray analysis was found to be around 15Å and the IQHs are shown to be made up of circular disks each corresponding to a particular in-plane lattice parameter. Two nearest IQHs are typically separated by 600Å as observed in the XTEM data. The average diameters of the various disks as obtained from the x-ray study are also indicated. The $Si_{1-x}Ge_x$ composition gradient in each of these disks is shown by the color gradation. The dark color at the rim and tip regions correspond to the presence of higher Ge content ($Si_{0.7}Ge_{0.3}$) as compared to the central lighter region having a rather lower Ge content ($Si_{0.8}Ge_{0.2}$). It is to be noted here that x-ray measurements provide spatially averaged information as compared to the XTEM measurements that provide localized information about a typical IQH present in the system. The information obtained from the x-ray scattering study regarding the average size, composition and strain profile of the IQH structures was found to be consistent with the XTEM results. The intriguing composition variation within IQH lead to a very low strain value of 1.66% between the rim structure and the vicinal Si [13]. We shall discuss here the effect of this

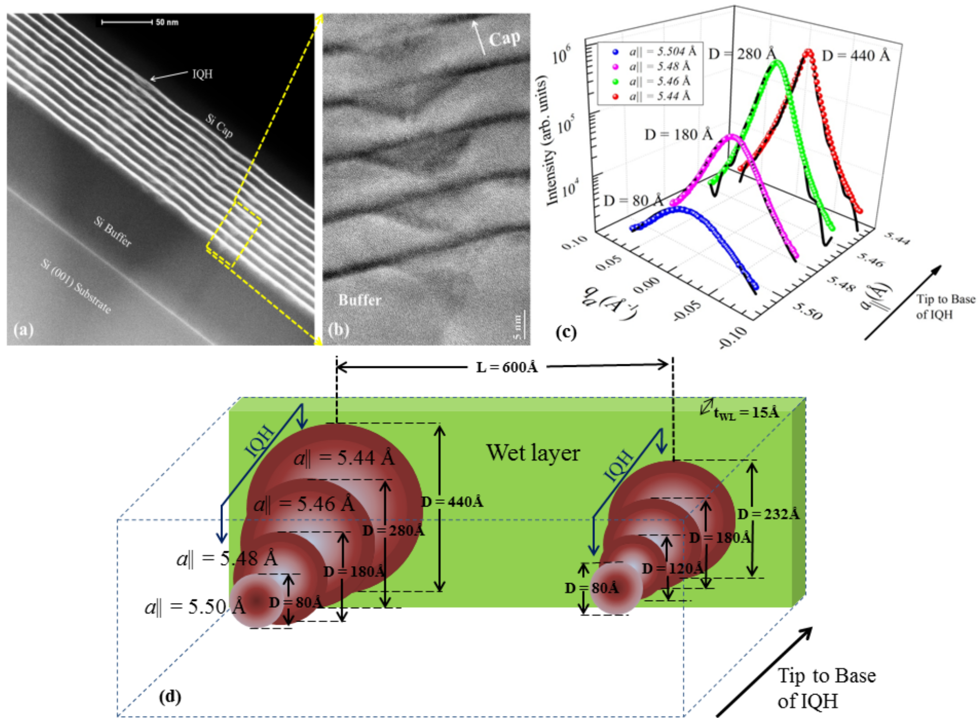

Fig. 1 (a) HAADF image of IQH embedded superlattice structure. Vertical alignment of IQH in various layers is evident. (b) High resolution XTEM image of self-organized IQHs embedded in the superlattice structure. (c) Typical angular scans around (400) of the IQH embedded superlattice structure measured at 11 043eV. Each scan is associated with a different $a_{\|}$. The solid lines show fits assuming the IQH to be composed of four disks each having a unique in-plane lattice parameter. The diameter of the disks for different $a_{\|}$ is indicated. (d) Schematic showing a typical bilayer consisting of IQH structures. The various dimensions (as indicated) represent the results obtained from the analysis of x-ray data.

low strain value on the optical properties of these superlattices.

3 Results and Discussion

Temperature and excitation power dependent PL measurements were performed in a closed-cycle helium cryostat having temperature range from 10 to 300K, with a 980nm semiconductor laser. The PL spectra were recorded by a liquid nitrogen cooled InGaAs detector using standard lock-in technique.

3.1 Temperature dependent PL

Figure 2(a) shows the temperature dependent PL spectra taken at an excitation power of 40mW. The PL signal is observed to be very broad even at low temperatures. The PL spectra from 10 to 50 K have been analyzed using three gaussian curves and the fitted profiles are shown by the dash-dot lines for the 10K spectrum in Figure 2(a). Thus, a combined contribution from three different PL peaks having their centers positioned around 0.81, 0.87 and 0.92eV leads to a broad PL intensity. The PL emission peak at 0.81eV can be attributed to the confinement of charge-carriers in the IQH structure. The PL from Ge IQH is not phonon-assisted, hence it corresponds to direct band-gap. The peaks at 0.92 and 0.87eV are the no-phonon (NP_{WL}) and its transverse-optic (TO_{WL}) replica respectively which occur due to the exciton confinement in the wet layer [14]. This peak position for wet layer corresponds to a thickness of around 4.5ML [14] which matches quite well with the thickness of nearly 6Å having maximum Ge content of $Si_{0.6}Ge_{0.4}$ of the present sample. These two peaks are 49meV apart and hence correspond to Si-Ge optical phonon energy peak [15]. The FWHM of the IQH related PL emission peak at 0.81eV is observed to be around 90meV. It is to be noted that width of similar PL emission peaks for conventional Ge quantum dots was found to be around 70meV [16].

The temperature dependence of the three PL peak energies is shown in Figure 2(b). The peak positions of wet-layer related PL remain invariant with the rise in temperature from 10 to 50K and this emission quenches for higher temperatures. Figure 2(c) shows the variation of integrated PL intensities (I_{PL}) with the change in temperature for the three PL peaks. The integrated

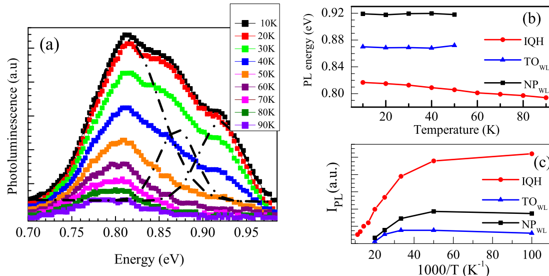

Fig. 2 (a) Temperature dependence of the PL spectra for the IQH embedded superlattice. The PL spectra at low temperature can be fitted using three gaussians as indicated by three dash-dot curves for 10K spectrum. Temperature dependence of PL (b) peak positions and (c) intensities of the three peaks corresponding to IQH, TO_{WL} and NP_{WL}. At higher temperatures (60K and above) only IQH related PL is observed.

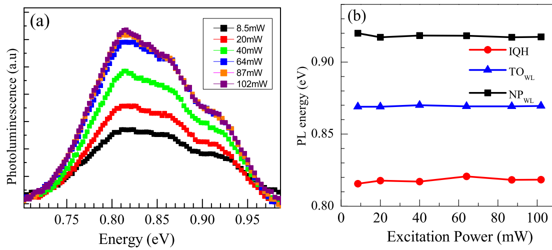

Fig. 3 (a) The excitation power dependent PL spectra at 10K. (b) The excitation power dependence of the PL energies for the three emissions at 10K.

PL intensities (I_{PL}) for all the three peaks are seen to decrease with rise in temperature. This shows that the bound-excitons attain thermal energy to escape the bound-state and recombine non-radiatively as the temperature increases.

3.2 Excitation power dependent PL

Excitation power dependent measurements were performed at 10K and the results are shown in Figure 3(a). A shift in the peak emission energy depends upon the type of band lineup present in the system. It is well documented that conventional Ge QD grown above Ge wet layer exhibit Type II band-alignment, where carriers are trapped in the notch potential of strained Si/Ge interface, with holes inside the Ge and electrons inside the Si region. These spatially separated charge carriers build up an electrostatic potential which bends the energy-bands [17] as the carrier concentration increases with the increased excitation power. In conventional QD system, the Si conduction band-bending shifts the electrons to higher energies due to increased confinement in the notch potential that leads to a blue shift in the PL emission energy [18]. However, Ge IQH structures presented here have exhibited considerably lower interfacial strain and the effect of cap layer can be neglected here. We have found here that with the variation in pump power, the peak positions of all the transitions remain almost unaltered [refer Figure 3(b)]. This shows that the transitions related to these PL emissions are not Type-II and no band-bending is induced with the increase in excitation power. These measurements were performed at 30K and 50K as well. At higher temperature also, no change in the emitted PL energy with excitation power was observed. Self-assembled growth of the IQH structures with SiGe alloying within Si (001) lattice reduces the strain considerably and hence reduces the conduction band offset [17]. Hence, position of PL of the IQH structures was found to be independent of excitation power as has been observed previously in annealed Ge quantum dot samples [7].

The thermal activation energy for the IQH related peak can be calculated by following equation [18]:

$$I_0/I_{PL}(T) = 1 + C_1 e^{(-E_1/kT)} + C_2 e^{(-E_2/kT)} \quad (1)$$

where I_0 is the maximum intensity, E_1 and E_2 are the thermal activation energies, C_1 and C_2 are fitting parameters and k is Boltzmann's constant. In Figure 4(a) we have shown the fitted variation of I_0/I_{PL} of IQH emission as a function of temperature to reveal the role of two activation energies 12.2 and 51.6meV. The activation energy of 12.2meV contributes only in the low-temperature region and that of 51.6meV correspond to higher temperatures. It is interesting to note that the activation energy of 51.6meV corresponds to a carrier confinement dimension of 70Å [16] which is nearly the size of the tip of IQH structures as obtained from the XTEM and x-ray studies. Thus, this activation energy of 51.6meV corresponds to the tip region of the IQH and that of 12.2meV is due to confinement of carriers in the base region of IQH. As the temperature increases, the bound excitons dissociate into free or non-correlated pairs of electron and holes which lead to a decrease in the PL intensity. From XTEM and x-ray studies, it is known that the density of IQH in the superlattice system is very low and only 15% of total Ge resides in them while rest of the Ge belongs to the wet layer. Despite the very low Ge content, the IQH show very high PL emission due to the exciton confinement in these structures.

The PL peak originated from IQH shifts the energy position from 0.81 to 0.79eV as the temperature is raised from 10 to 90K. The temperature dependence of this band-gap related emission can be approximated by Varshni's equation [19] given by $E(T) = E_g - (\alpha T^2)/(T + \beta)$ as shown in Figure 4(b), where $\alpha = 0.0012$eV/K and $\beta = 210$K. E_g is the band-gap at 0K and is found to

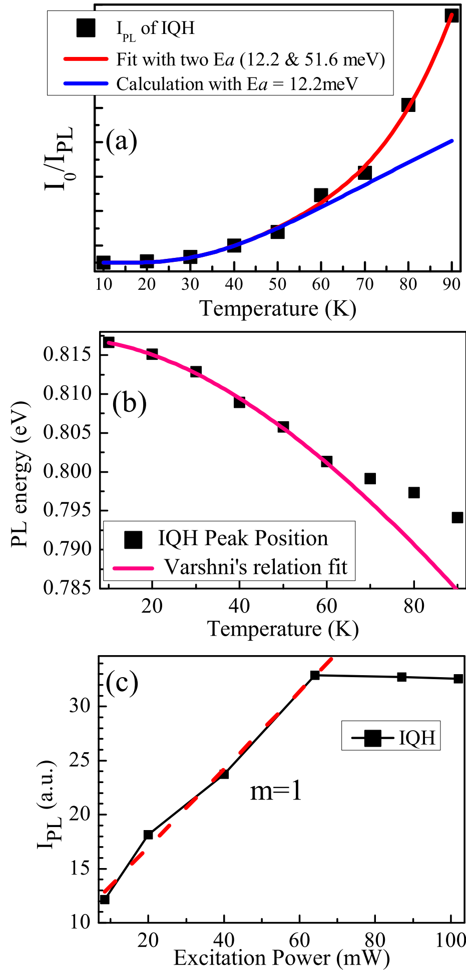

Fig. 4 (a) I_0/I_{PL} versus temperature plot for IQH related emission. The line profile represents the fit considering two activation energies (12.2 and 51.6meV). Also, calculation of the intensity variation is shown for activation energy of 12.2meV. (b) Temperature variation of PL peak position and fit by Varshni's relation for IQH related emission. (c) Variation of integrated PL intensity for the IQH related peak with excitation power. The dash-line profile represent the power law (I_{PL}) fit and the corresponding power exponent is indicated.

be 0.82eV. It should be noted that the IQH peak follows Varshni's relation only in the low temperature region and at high temperatures, the IQH indicate higher band-gap than expected by Varshni's relation. It is to be noted here that atom-like levels expected in quantum structures may not show variation of 'band-gap' with temperature. Figure 4(c) shows the variation of integrated PL intensity (I_{PL}) with the excitation power for the IQH related PL emission. It is observed that the I_{PL} first increases with excitation power and then abruptly saturates above 64mW excitation power.

4 Conclusions

We have presented here results of a photoluminescence study of MBE grown SiGe superlattice structures having inverted quantum huts with high Ge content formed below Ge-on-Si interfaces. Unlike conventional Ge quantum dots formed above Ge-on-Si interfaces, the presented quantum structures exhibit excitation-power independent photoluminescence energy. It is known that the intensity depends on excitation as $I \propto P^m$ where 'I' represents the PL intensity and 'P' the excitation power, the exponent 'm' is found to be 1 for this IQH related PL emission which further indicates the band-alignment to be Type-I. The saturation of the peak intensities can be attributed to the filling of finite density of states in the IQH and wet layer as the excitation energy used here was not high enough. The presented results may play a significant role in the development of silicon based optical materials. However further studies are required to establish that the observed PL is of Type-I.

Acknowledgements Authors would like to acknowledge the support of Department of Science and Technology (DST) for carrying out synchrotron experiments at Petra III, DESY, Germany through the DST-DESY project operated through Saha Institute of Nuclear Physics.

References

1. G. D. Scholes, G. Rumbles, Excitons in nanoscale systems, Nat. Mat. 5, 683 (2006).
2. T. P. Pearsall, J. Bevk, L. C. Feldman, J. M. Bonar, J. P. Mannaerts, A. Ourmazds, Structurally Induced Optical Transitions in Ge-Si Superlattices, Phys. Rev. Lett. 58, 729 (1987).
3. M. Kumagai, T. Takagahara, E. Hanamura, Optical properties and indirect-to-direct transition of GaP/AlP (001) superlattices, Phys. Rev. B, 37, 898 (1988).
4. D. Grutzmacher, T. Fromherz, C. Dais, J. Stangl, E. Muller, Y. Ekinci, H. H. Solak, H. Sigg, R. T. Lechner, E. Wintersberger, S. Birner, V. Holy, G. Bauer, Three-Dimensional Si/Ge Quantum Dot Crystals, Nanolett. 7, 3150 (2007).
5. K. Brunner, Si/Ge nanostructures, Rep. Prog. Phys. 65, 27 (2002).
6. J. Wan, G. L. Jin, Z. M. Jiang, Y. H. Luo, J. L. Liu, K. L. Wang, Band alignments and photon-induced carrier transfer from wetting layers to Ge islands grown on Si(001), Appl. Phys. Lett. 78, 1763 (2001).
7. J. Wan, Y. H. Luo, Z. M. Jiang, G. Jin, J. L. Liu, Kang L. Wang, X. Z. Liao and J. Zou, Effects of interdiffusion on the band alignment of GeSi dots, Appl. Phys. Lett. 79, 1980 (2001).
8. C. G. V. Walle, R. M. Martin, Theoretical calculations of heterojunction discontinuities in the Si/Ge system, Phys. Rev. B, 34, 5621 (1986).
9. J. Tersoff, C. Teichert, M. G. Lagally, Self-Organization in Growth of Quantum Dot Superlattices, Phys. Rev. Lett. 76, 1675 (1996).

10. V. L. Thanh, V. Yam, P. Boucaud, F. Fortuna, C. Ulysse, D. Bouchier, L. Vervoort, J. -M. Lourtioz, Vertically self-organized Ge/Si(001) quantum dots in multilayer structures, Phys. Rev. B, 60, 5851 (1999).
11. Y. L. Soo, G. Kioseoglou, S. Huang, S. Kim, Y. H. Kao, Y. H. Peng, H. H. Cheng, "Inverted hut" structure of Si-Ge nanocrystals studied by extended x-ray absorption fine structure method, Appl. Phys. Lett. 78, 3684 (2001).
12. H. H. Cheng, W. P. Huang, V. I. Mashanov, G. Sun, Local intermixing on Ge/Si heterostructures at low temperature growth, J. Appl. Phys. 108, 044314 (2010).
13. M. Sharma, M. K. Sanyal, B. Satpati, S. K. Ray, Anomalous x-ray scattering study of the growth of inverted quantum hut structures in a Si-Ge superlattice emitting strong photoluminescence, Phys. Rev. B, 89, 205304 (2014).
14. M. Brehm, M. Grydlik, H. Groiss, F. Hackl, F. Schaffler, T. Fromherz, G. Bauer, The influence of a Si cap on self-organized SiGe islands and the underlying wetting layer, J. Appl. Phys. 109, 123505 (2011).
15. M-Y. Ryu, T. R. Harris, Y. K. Yeo, R. T. Beeier, J. Kouvetakis, Temperature-dependent photoluminescence of Ge/Si and Ge1-ySny/Si indicating possible indirect-to-direct bandgap transition at lower Sn content, Appl. Phys. Lett. 102, 171908 (2013).
16. C. S. Peng, Q. Huang, W. Q. Cheng, J. M. Zhou, Y. H. Zhang, T. T. Sheng, C. H. Tung, Optical properties of Ge self-organized quantum dots in Si, Phys. Rev. B, 57, 8805 (1998).
17. J. Weber, M. I. Alonso, Near-band-gap photoluminescence of Si-Ge alloys, Phys. Rev. B, 40, 5683 (1989).
18. M. Larsson, A. Elfving, W. X. Ni, G. V. Hansson, P. O. Holtz, Growth-temperature-dependent band alignment in Si/Ge quantum dots from photoluminescence spectroscopy, Phys. Rev. B, 73, 195319 (2006).
19. H. Yang, Z. Tao, J. Lin, F. Lu, Z. Jiang, Z. Zhong, Systematic studies of the photoluminescence of Ge quantum dots grown on strained Si0.7Ge0.3 buffer layer, Appl. Phys. Lett. 92, 111907 (2008).